

DEVELOPMENT OF HIGH FIELD DIPOLE MAGNET AND POWER SUPPLY FOR PROTON THERAPY

K. Endo and K. Egawa, KEK, Tsukuba, Japan

Z. Fang, NIRS & KEK, Chiba, Japan

M. Mizobata and I. Uchiki, Mitsubishi Electric Corp., Kobe, Japan

Abstract

A small dipole magnet of 3 T and its pulsed power supply feeding 200 kA at maximum are being developed for the table-top proton synchrotron for the proton-therapy. The experimental field distribution is consistent with the 3D dynamic field simulation. The dipole field was measured at the time interval of 2 μ sec with 15 tiny search coils aligned accurately to the radial direction at 5 mm pitch. The dipole is excited by the discharge current of the capacitor bank of 200 kJ with the rise time of about 5 msec. Performances of the dipole and power supply are described with the numerical simulations.

INTRODUCTION

The dedicated medical proton accelerators are designed to have a maximum energy of 250 MeV or slightly more, however, in most cases about 80% of patients could be treated with the proton energy less than 200 MeV guessing from the maximum tumor depth distribution treated so far [1]. The radiotherapy using accelerated protons and/or heavy ions is recognized as an effective method to cure the malignant tumor offering the QOL (quality of life). It is now in an aged society especially important to promote this advanced method countrywide and/or worldwide. Several dedicated proton accelerators (synchrotron and cyclotron) are built and used at the medical centers. However, they are not enough to treat all patients who really want the advanced radiotherapy. So far the accelerator itself is very expensive and requires the special facility to install. To promote this radiotherapy in a reasonable cost, the smaller and cheaper accelerator but limited in the maximum energy is desired to develop. The compact accelerators serve as complements to the large facility and will enhance the advanced cancer treatment at the residential districts.

Synchrotron is convenient to change the beam energy from pulse to pulse if the treatment depth to the patient is required to control locally to avoid the dose to the normal tissue. To make the proton synchrotron of 200 MeV for the radiation therapy small enough for installation and convenient for the daily clinical treatment in the hospital environment, the development of the high field compact dipole magnet with performance of the accelerator grade is indispensable [2, 3, 4]. Another requirement to the compact ring is to reduce the overall longitudinal dimension of the RF cavity with the average accelerating gradient of ~ 40 kV/m [5]. Its RF frequency range is well wide and the accelerating voltage is very large to

accomplish the acceleration within the duration while the ohmic heat dissipation can allow the temperature rise of the dipole coil. The RF issues are treated by the paper of this conference [6].

According to the size of the horizontal beam aperture, the cross-sectional dimensions of the dipole become large. If they are limited by the ring size, the iron core saturation becomes large when attaining a high magnetic field. There is a room for a trade off between the maximum field strength and the beam aperture. The present optics design has a preference to the beam aperture so as to obtain the sufficient beam intensity extracted for the medical treatment. The peak field of the dipole is suppressed to 3 T at 200 MeV, however, the dipole core saturates considerably.

The pulsed power supply was also manufactured. It has a base on the charge/discharge of the energy storage capacitor. The discharge current steps up through the pulse transformer to attain the peak current of 200 kA corresponding to the dipole field of 3 T. The power supply and the dipole magnet compose a resonant circuit of which rise time is used for the acceleration [7].

PARAMETERS OF 2 LATTICE VERSIONS

Main machine parameters are given in Table 1 with the revised parameters for the missing quadrupole version and their layouts are shown in Fig.1. The joint design study by BINP and Frascati is also given for reference. Each design has the different dispersion and the horizontal/vertical tunes depending on the cell structure. Present lattices are FODOFB with small dispersion at the dipole magnet and DOB with the reduced circumference. Either lattice has the same dipole magnet parameters.

Table 1: Parameters for 200 MeV proton synchrotron.

	BINP/Frascati	KEK		unit
Max. energy	200.0	200.0	200.0	MeV
Inj. energy	12.0	2.0	2.0	MeV
Circumference	6.4	11.9	9.5	m
Av. diameter	2.0	3.6	3.0	m
Bending radius	0.54	0.72	0.72	m
Max. dipole field	4.0	3.0	3.0	T
Period	4	4	4	
Tune, Q_x/Q_y	1.42/0.54	2.25/1.25	1.6/0.6	
Max. dispersion	0.63	0.5	0.8	m
Cell structure	BODO	FODOFB	DOB	
Frequency range	7.4~26.5	1.9~16.2	2-18	MHz
Acc. voltage	12.4	13.0	13.0	kV
Acc. time	3.5	5.0	5.0	msec

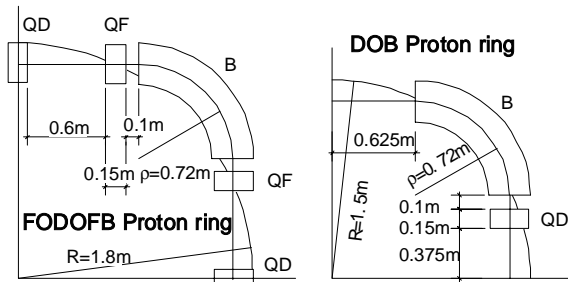


Figure 1: Layouts of the compact proton synchrotron (FODOFB and DOB versions).

DIPOLE MAGNET AND PERFORMANCE

The ring consists of 4 dipole magnets which are serially connected with the pulsed power supply of 200 kA at peak. A prototype dipole magnet whose cross-section is shown in Fig.2 was designed by using the time-dependent 3D simulation code. The pole end profile was also simulated approximating the continuous curvature (Rogowsky curve) or the slant plane by the horizontal steps as shown in Fig.3. According to simulations both ends of the pole extending 5 cm from the core edges are tapered to attain a uniform effective dipole length as shown in Fig.4 and the completed dipole magnet is given in Fig.5.

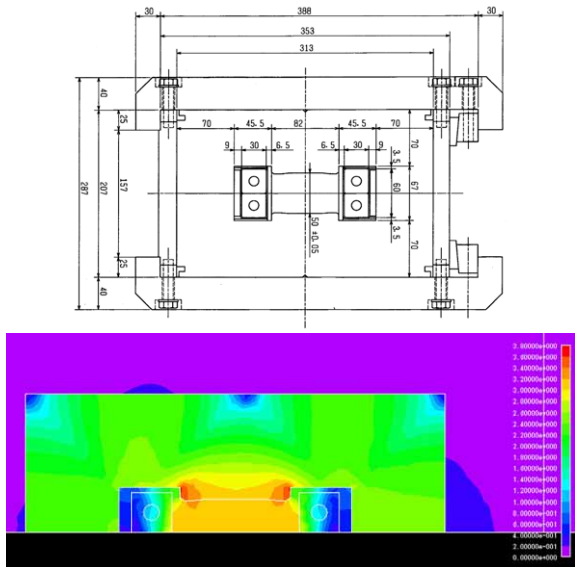


Figure 2: Cross-sectional dimensions of the dipole (top), and field distribution at max. excitation (bottom).

The field distribution is measured by using 15 search coils precisely aligned to the radial direction in the probe holder which are moved manually at every 0.9 or 0.45 deg. step on the field measuring table on which the many precise pin holes are drilled to align the probe at the exact positions by inserting a pin. Induced 15 voltages are saved at every 2 μ sec and integrated to convert them to the field data with a personal computer. The field distributions normalized at the center of the dipole are given in Fig.6 with the results of the field calculation.

The experimental data reproduce fairly well the numerically obtained distributions. The effective magnet length along the central orbit is given in Fig.7. At low field the effective length is longer by about 20 mm than the simulation. The time base differs between the calculation and measurement because the real magnet excitation depends on the resonant condition of the circuit. So the experimental time base is shortened by adjusting the measured current to that of calculation.

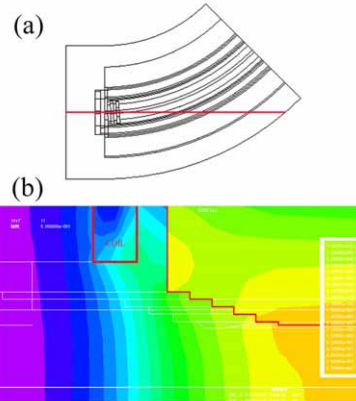


Figure 3: Pole end profile for the field calculation. (a) Plan view of the half dipole and cut plane, (b) the pole end profile and the field distribution by the color codes on the cut plane.

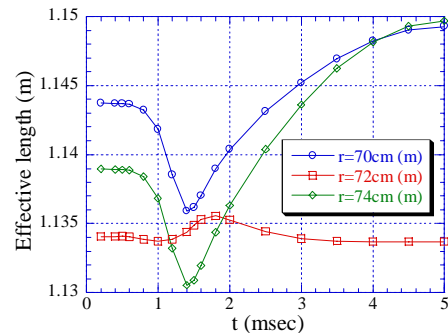


Figure 4: Numerically obtained effective length as a function of time. The squares correspond to the central orbit. The others are those at ± 2 cm.



Figure 5: Completed dipole magnet connection to the pulse transformer with a bus-bar.

The effective magnet length is obtained by integrating the measured field map numerically on the gap medium plane. As the search coil moves on the field measuring

table to form a circular arc both inside and outside of the dipole. However, at the outside of the magnet the integration should be taken along the tangential line on which the magnetic field was interpolated by the method of an iso-parametric transformation in conjunction with the generalized matrix inversion.

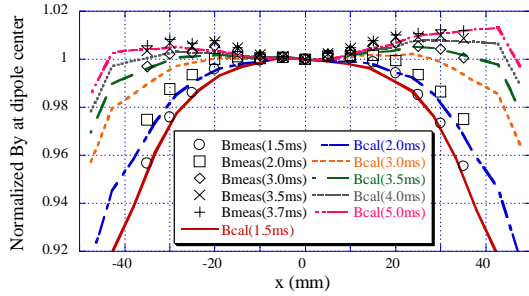


Figure 6: Measured and calculated field distributions.

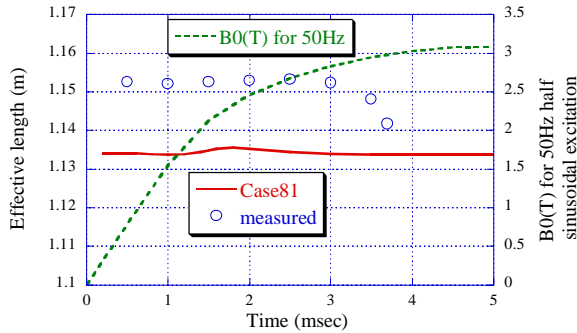


Figure 7: Measured and calculated (Case81) effective magnet length.

PULSED POWER SUPPLY

To generate 3 T in the gap of 5 cm in height with a single turn coil, the excitation current is as large as 200 kA. The coil dimensions are small because of the compact construction of the dipole magnet. The cooling capacity of the heat dissipated during the excitation determines the current pulse width. Assuming the sinusoidal excitation with a peak current I_p and a pulse rate η repetitions/sec, the effective current is $I_{eff} = 0.5I_p\sqrt{\eta/f}$ for the rise and fall time equivalent to f Hz. As this case is equivalent to 50 Hz, $I_{eff} = 14.1\sqrt{\eta}$ [kA]. In practice, the current differs from the sinusoidal pattern due to the saturation of the magnet and the repetition rate is 5 Hz or less depending on the coil temperature. To avoid the skin effect the coil is made of the strand Cu cable impregnated with the epoxy resin of which thermal conductivity is considerably so low to allow only 1 Hz repetition rate. To improve this situation, it will be considered to replace the coil with that made of the OFC hollow conductor after the study.

As the discharge current of the capacitor bank is utilized to excite the dipole, the tracking control is made by the precise current control of the quad after the dipole current which serves as a reference signal to the quad power supply. This kind of control is relatively easy because the quad current is about one tenth of the dipole current or less for the DOB lattice version.

The power supply shown in Fig.8 has the capacitor bank (10 mF, 6.5 kV) to excite 4 dipoles.

Before manufacturing the pulsed power supply, the charge, discharge and residual energy recovery circuits are simulated using PSpice code for all dipoles serially connected. The current pulse width is adjusted to 10 msec (50 Hz equivalent) by changing the circuit parameters such as the pulse transformer winding ratio, capacitor, charging voltage and etc. The measured current pulse and the central dipole field are plotted in Fig.9 when the energy recovery circuit is working.

Authors greatly acknowledge a favor of Prof. Y. Hirao and Dr. S. Yamada of NIRS to perform this work.



Figure 8: Completed pulse power supply for dipole magnets. From left to right; charging block, control block, 200 kJ capacitor bank, discharge block and pulse transformer (shown in Fig.1).

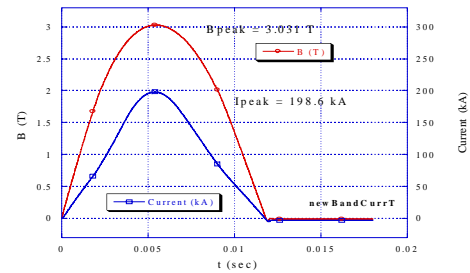


Figure 9: Measured time-dependent excitation curve.

REFERENCES

- [1] Y. Hirao, "Results from HIMAC and Other Therapy Facilities in Japan," Proc. Cyclotrons 2001, pp.8-12.
- [2] K. Endo et al, "Compact Proton and Carbon Ion Synchrotron for Radiation Therapy," Proc. EPAC2002, Paris, pp.2733-5.
- [3] K. Endo et al, "Development of High Field Dipole and High Current Pulse Power Supply for Compact Proton Synchrotron," PAC'03, Portland, to be published.
- [4] K. Endo et al, "Development of Compact Proton Synchrotron for Radiation Therapy," ARTA2003, Tokyo, to be published.
- [5] Z. Fang et al, "RF Cavities and Power Amplifier for the Compact Proton Synchrotron," PAC'03, Portland, to be published.
- [6] Z. Fang et al, "RF Cavity for Table-Top Proton Synchrotron," this conference.
- [7] K. Endo et al, "Resonant Pulse Power Supply for Compact Proton and/or Heavy Ion Synchrotron," Proc. APAC2001, Beijing, pp.636-8.